Feasibility of ^{18}F-FDG PET as a Noninvasive Diagnostic Tool of Muscle Denervation: A Preliminary Study

Seung Hak Lee[1], Byung-Mo Oh[1], Gangpyo Lee[1], Hongyoon Choi[2], Gi Jeong Cheon[2], and Shi-Uk Lee[3]

[1]Department of Rehabilitation Medicine, Seoul National University Hospital, Seoul, South Korea; [2]Department of Nuclear Medicine, Seoul National University Hospital, Seoul, South Korea; and [3]Department of Rehabilitation Medicine, Seoul National University Boramae Medical Center, Seoul, South Korea

The purpose of this study was to confirm glucose hypermetabolism in denervated muscle and investigate the feasibility of ^{18}F-FDG PET scanning for the detection of muscle denervation. **Method:** A sciatic neuropathy model in rats was created by nerve resection of the left sciatic nerve and sham operation on the other side. Eight days after denervation, small-animal PET/CT scans of the hindlimbs were acquired. Muscle denervation was confirmed by electrophysiologic and histologic study. **Results:** All rats showed increased ^{18}F-FDG uptake in the muscles of the left (denervated) lower legs. The calculated maximum lesion-to-normal counts ratio of the left lower leg anterolateral (left, 11.02 ± 2.08; right, 1.81 ± 0.40, $n = 6$, $P < 0.01$) and posterior (left, 9.81 ± 4.58; right, 1.87 ± 0.44, $n = 6$, $P < 0.01$) compartment were significantly increased. The electrophysiologic and histologic study verified muscle denervation. **Conclusion:** Glucose hypermetabolism in muscle denervation is an obvious phenomenon. ^{18}F-FDG PET scanning can be used to visualize muscle denervation.

Key Words: muscle denervations; ^{18}F-FDG; sciatic neuropathies; positron emission tomography

J Nucl Med 2014; 55:1737–1740
DOI: 10.2967/jnumed.114.140731

Needle electromyography was the first electrophysiologic technique to evaluate peripheral neuromuscular disorder; it has been used as a main electrodiagnostic tool (*1*). Electromyography can detect muscle denervation resulting from various causes, such as trauma, neuropathies, and neoplasm. Although needle electromyography is currently considered as a standard test, it is an invasive and painful procedure for patients (*2*). Therefore, a new noninvasive diagnostic modality would be of great use. MR imaging can visualize acute and subacutely denervated muscles through high signal intensity of the muscle in fluid-sensitive MR sequences (*3,4*). Furthermore, MR imaging mirrors the electrophysiologic changes after denervation and also has several advantages, including the ability to detect an injured nerve itself (*3,4*). However, MR imaging has not been a routine study to evaluate muscle denervation and therefore cannot substitute for electromyography. Recently, increased ^{18}F-FDG uptake in the denervated muscle was reported incidentally (*5*). To our knowledge, there has not been a study that explored a direct correlation between muscle denervation and increased ^{18}F-FDG uptake. The purpose of this study was to confirm glucose hypermetabolism in a denervated muscle using a sciatic nerve injury rat model and to investigate the feasibility of ^{18}F-FDG PET scanning as a noninvasive diagnostic tool for muscle denervation.

Received Mar. 26, 2014; revision accepted Jul. 17, 2014.
For correspondence or reprints contact: Shi-Uk Lee, Department of Rehabilitation Medicine, Seoul National University College of Medicine, Department of Rehabilitation Medicine, Seoul National University Boramae Medical Center, 425, Sindaebang-dong, Dongjak-gu, Seoul, South Korea, 156-707.
E-mail: shiuk.lee@gmail.com
Published online Aug. 7, 2014.

MATERIALS AND METHODS

Animal Model

Six male Sprague–Dawley rats (7 wk old) were used. They were anesthetized, and the left sciatic nerve was exposed by splitting the gluteal muscles. A 10-mm nerve segment was resected just proximal to the bifurcation into the common peroneal and tibial nerves. Sham operation, exposing the sciatic nerve without resection, was performed on the right side of the rats. Additionally, one more rat was used for a tibial neuropathy model by resection of the left tibial division of the sciatic nerve around the bifurcation level with microscopic assistance, sparing the peroneal division. The experimental protocol was approved by the Institutional Animal Care and Use Committee (IACUC) of Seoul National University Hospital (IACUC approval no. 13-0203).

^{18}F-FDG PET/CT

The rats were scanned with a small-animal PET/CT system (eXplore VISTA; GE Healthcare) 8 d after the denervation. For the PET scans, 37 MBq of ^{18}F-FDG was injected intravenously. The animals were anesthetized with isoflurane inhalation on a warmed platform for 1 h, immediately after ^{18}F-FDG injection. Then the rats were kept anesthetized and fixed to a wooden animal holder and underwent small-animal PET/CT. A 20-min static PET scan of the hindlimbs was acquired, and a CT scan followed immediately after.

The size of the reconstructed voxel was $0.3875 \times 0.3875 \times 0.675$ mm. Regions of interest (ROIs) for both sides of the anterolateral and posterior compartment muscles of the lower legs were drawn manually along with the boundary of each compartment. These ROIs were drawn in the axial section, at the mid-lower-leg level, which showed prominent ^{18}F-FDG uptake. CT overlay images provided anatomic guidance (Fig. 1A). To normalize ^{18}F-FDG uptake in the ROIs, we used additional ROIs on both sides of the upper thigh muscles, which were not affected by surgery. These were drawn in the axial section and were disk-shaped; the diameters were 7 mm for all ROIs (Fig. 1A). Then we calculated the maximum lesion-to-normal counts ratio (LNR_{max}), defined as the maximal count of each compartment ROIs divided by the average of mean count of both upper thigh ROIs.

Electrophysiologic Study, Histology, and Molecular Study

Rats underwent nerve conduction study (NCS) and electromyography on day 9, under anesthesia. Compound motor action potentials of

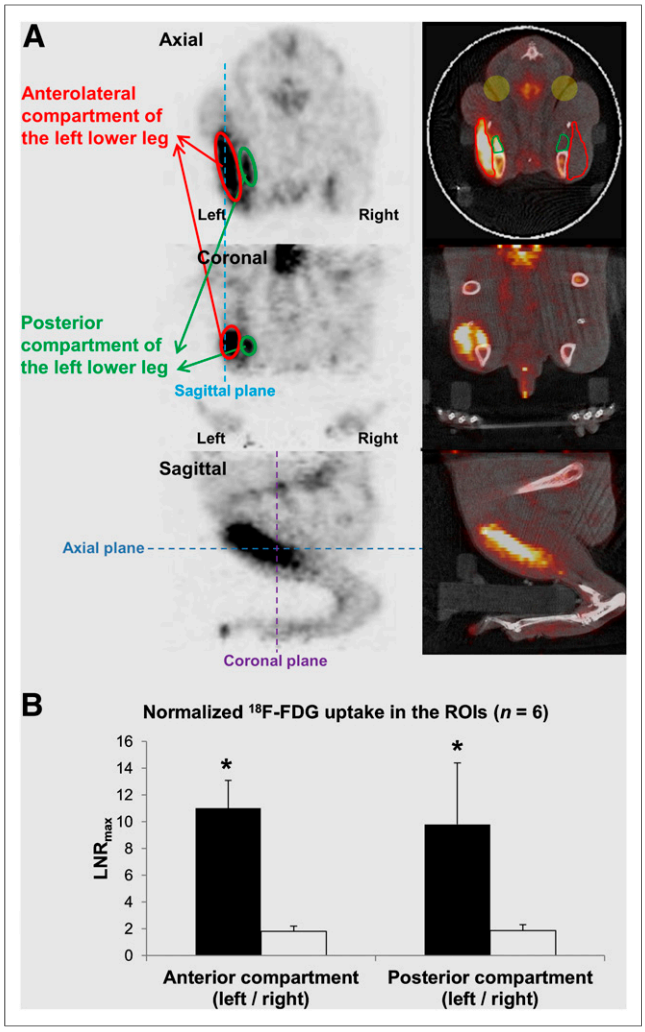

FIGURE 1. ^{18}F-FDG PET scans of hindlimbs of rat models, 8 d after denervation. (A) Images of axial, coronal, and sagittal sections are shown. PET/CT overlay fusion images are shown on right side. ROIs for each compartment are drawn in axial section of fusion image, red line for anterolateral and green line for posterior, respectively. ROIs for both upper thigh are drawn in transparent yellow circles, which cannot be drawn on provided axial image because of its rostral location. Increased radioactivities of denervated left anterolateral and posterior compartments muscles are shown. (B) LNR_{max} values are significantly increased at left side for both compartments. *$P < 0.01$.

both lower legs and feet intrinsic muscles were obtained. Needle electromyographies were performed on both lower leg muscles. Immediately after NCS and electromyography, the rats were euthanized. Tissue samples were obtained from both sides of the lower leg muscles. Standard hematoxylin and eosin stain and immunohistochemistry for glucose transporter 1 (GLUT-1), glucose transporter 4 (GLUT-4), and hexokinase II were performed. Western blots of each protein were performed, and normalized optical densities were measured with an imaging software (freeware ImageJ [http://imagej.nih.gov/ij/]) for quantification. Glyceraldehyde 3-phosphate dehydrogenase (GAPDH) was used for normalization.

Statistical Analysis

Wilcoxon signed-rank tests were performed to detect the difference of LNR_{max} and normalized optical density, between the denervation side and sham-operation side. A P value of 0.05 was set to assess their statistical significance.

RESULTS

^{18}F-FDG PET/CT scans showed increased ^{18}F-FDG uptake in the left anterolateral and posterior compartment muscles of the lower legs, 8 d after the denervation (Fig. 1A). The mean LNR_{max} of the denervated side (left) was significantly increased in comparison to the sham-operation (right) side in both the anterolateral (left, 11.02 ± 2.08; right, 1.81 ± 0.40, $n = 6$, $P < 0.01$) and the posterior (left, 9.81 ± 4.58; right, 1.87 ± 0.44, $n = 6$, $P < 0.01$) compartments (Fig. 1B). In all rats, the needle electromyography revealed abundant abnormal spontaneous activities in the denervated muscles, and compound motor action potentials were not evoked on NCSs, which were compatible with complete left sciatic neuropathy. Hematoxylin and eosin stain of the left gastrocnemius and tibialis anterior showed minimal neurogenic atrophy (small angulated fibers), which was compatible with denervation. Immunohistochemistry (Fig. 2) and Western blots (Fig. 3) revealed an increased expression of GLUT-1 in the denervated gastrocnemius muscle (left, 1.41 ± 0.34; right, 0.98 ± 0.33, $n = 6$, $P < 0.01$) and hexokinase II in the denervated tibialis anterior muscle (left, 6.20 ± 3.61; right, 2.05 ± 1.21, $n = 6$, $P < 0.01$) with statistical significance. On the other hand, the expressions of GLUT-4 were decreased in the denervated muscles, compared with the control side, which was not statistically significant. From the tibial neuropathy model, only the posterior compartment muscles, which are innervated by the tibial division of the sciatic nerve, showed increased ^{18}F-FDG uptake (Fig. 4). Electromyography and NCS were compatible with complete left tibial neuropathy.

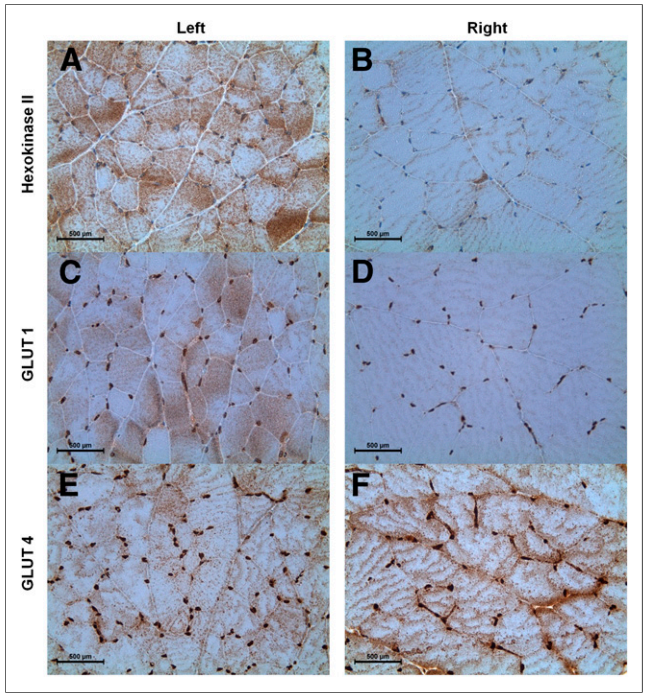

FIGURE 2. Results of immunohistochemistry from both gastrocnemius muscles. (A and B) Immunohistochemistry of hexokinase II shows increased expression of hexokinase II at left (denervated) side. (C and D) Immunohistochemistry of GLUT-1 shows increased expression of GLUT-1 at left side. (E and F) Immunohistochemistry of GLUT-4 shows no definite asymmetric expression. IHC = Immunohistochemistry.

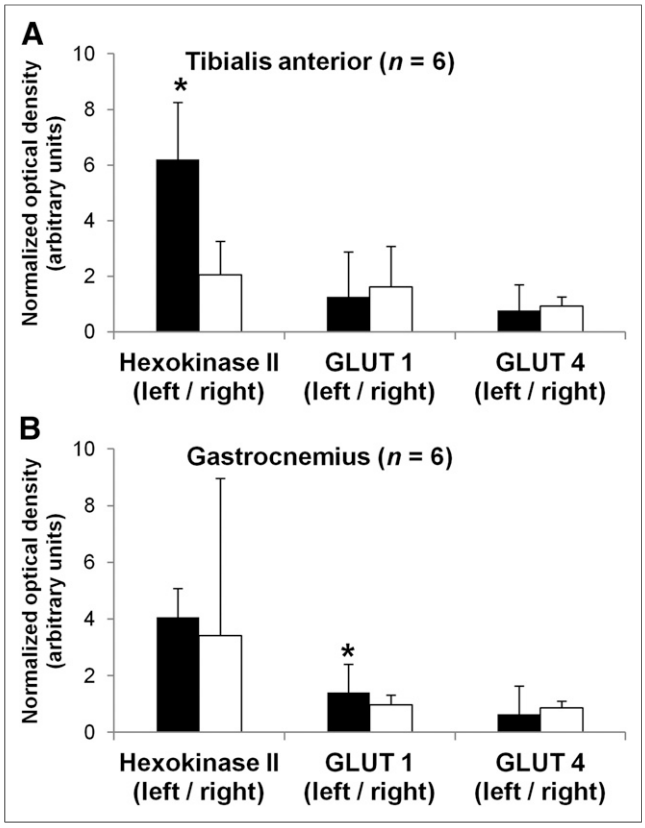

FIGURE 3. Results of Western blots. Normalized optical densities of hexokinase II in tibialis anterior muscle and GLUT-1 in gastrocnemius muscle are significantly increased in left (denervated) side, compared with sham-operation side. However, normalized optical densities of GLUT-4 in both gastrocnemius and tibialis anterior muscles are decreased without statistical significance. *$P < 0.01$.

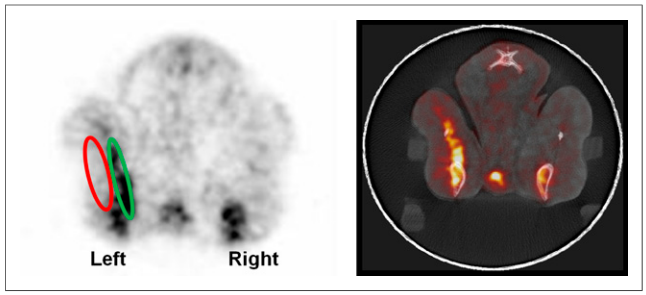

FIGURE 4. Axial images of left tibial neuropathy model. Anterolateral and posterior compartment are drawn with red and green circles, respectively. Only posterior compartment muscles show increased ^{18}F-FDG uptake, compared with Figure 1A.

DISCUSSION

This study confirmed increased glucose metabolism in denervated muscles with the ^{18}F-FDG PET scan, using a sciatic nerve injury model in rats. Muscle denervation was also verified with electrophysiologic and histologic studies. In our opinion, these findings are sufficient to confirm glucose hypermetabolism in denervated muscles.

The mechanism under this phenomenon is still unknown. Several hypotheses have been suggested. One hypothesis is that muscle denervation could be an energy-consuming process due to huge molecular changes. The results of immunohistochemistry and Western blots in this study were in agreement with previous researches. Block et al. reported that acute denervation (3–7 d after denervation) evokes decreased GLUT-4 expression and reciprocally increased GLUT-1 expression in rats (*6*). GLUT-4 is abundant in adult skeletal muscles; yet, GLUT-1 is mainly expressed in fetal skeletal muscles (*7*). Not only glucose transporters but also other cell membrane proteins, such as acetylcholine receptors (*8*), are also expressed as new embryonic forms in the denervated muscle. These changes are the molecular basis of the alteration in electrophysiology after denervation (*9*). Another possible hypothesis is apoptotic reaction in denervated skeletal muscles. Apoptosis has been considered as an energy-consuming process that can be accompanied by an ^{18}F-FDG uptake increase (*10*). There were several previous studies that have demonstrated that muscle denervation stimulates mitochondrially mediated apoptosis (*11*).

^{18}F-FDG is the most commonly used radiopharmaceutical of PET studies for cancer as well as for other diseases of the brain and heart (*12*). Skeletal muscles are not commonly evaluated by an ^{18}F-FDG PET scan, but there have been several studies on ^{18}F-FDG PET of skeletal muscles. Physiologic muscle contraction induces increased glucose metabolism, which can be used to evaluate and visualize skeletal muscle function with an ^{18}F-FDG PET scan (*13*). Nevertheless, clinical usefulness of ^{18}F-FDG PET scanning in peripheral neuromuscular disorder has not been established yet, except for musculoskeletal tumor (*14*). Moreover, ^{18}F-FDG uptake in the muscle has been regarded as a potential source of false-positive for PET scanning (*15*). Our experiment successfully visualized muscle denervation with ^{18}F-FDG PET/CT scanning, and thus it may suggest a new possible indication of ^{18}F-FDG PET study.

This research has provided many questions in need of further investigation. First, the molecular mechanism of glucose hypermetabolism in denervated muscles should be explored. Second, the temporal course of glucose hypermetabolism in denervated muscles and the relationship between the severity of nerve injury and the signal intensity of ^{18}F-FDG uptake should be investigated. Third, a comparison study on sensitivity and specificity between other modalities such as MR imaging and electrophysiologic studies during the denervation process is necessary.

CONCLUSION

Denervated muscle shows glucose hypermetabolism, and an ^{18}F-FDG PET scan may be used as a noninvasive modality for the evaluation of peripheral neuromuscular disorder. Further investigation is required.

DISCLOSURE

The costs of publication of this article were defrayed in part by the payment of page charges. Therefore, and solely to indicate this fact, this article is hereby marked “advertisement” in accordance with 18 USC section 1734. No potential conflict of interest relevant to this article was reported.

ACKNOWLEDGMENT

We thank Jin Joo Lee for assistance with the animal experiments.

REFERENCES

1. Daube JR, Rubin DI. Needle electromyography. *Muscle Nerve.* 2009;39:244–270.
2. Moon Y-E, Kim S-H, Choi W-H. Comparison of the effects of vapocoolant spray and topical anesthetic cream on pain during needle electromyography in the medial gastrocnemius. *Arch Phys Med Rehabil.* 2013;94:919–924.
3. Kamath S, Venkatanarasimha N, Walsh M, Hughes PM. MRI appearance of muscle denervation. *Skeletal Radiol.* 2008;37:397–404.
4. Wessig C, Koltzenburg M, Reiners K, Solymosi L, Bendszus M. Muscle magnetic resonance imaging of denervation and reinnervation: correlation with electrophysiology and histology. *Exp Neurol.* 2004;185:254–261.
5. Behera D, Jacobs KE, Behera S, Rosenberg J, Biswal S. ^{18}F-FDG PET/MRI can be used to identify injured peripheral nerves in a model of neuropathic pain. *J Nucl Med.* 2011;52:1308–1312.
6. Block NE, Menick DR, Robinson KA, Buse MG. Effect of denervation on the expression of two glucose transporter isoforms in rat hindlimb muscle. *J Clin Invest.* 1991;88:1546–1552.
7. Castelló A, Cadefau J, Cussó R, et al. GLUT-4 and GLUT-1 glucose transporter expression is differentially regulated by contractile activity in skeletal muscle. *J Biol Chem.* 1993;268:14998–15003.
8. Witzemann V, Sakmann B. Differential regulation of MyoD and myogenin mRNA levels by nerve induced muscle activity. *FEBS Lett.* 1991;282:259–264.
9. Midrio M. The denervated muscle: facts and hypotheses: a historical review. *Eur J Appl Physiol.* 2006;98:1–21.
10. Haberkorn U, Bellemann ME, Brix G, et al. Apoptosis and changes in glucose transport early after treatment of Morris hepatoma with gemcitabine. *Eur J Nucl Med.* 2001;28:418–425.
11. Muller FL, Song W, Jang YC, et al. Denervation-induced skeletal muscle atrophy is associated with increased mitochondrial ROS production. *Am J Physiol Regul Integr Comp Physiol.* 2007;293:R1159–R1168.
12. Fletcher JW, Djulbegovic B, Soares HP, et al. Recommendations on the use of ^{18}F-FDG PET in oncology. *J Nucl Med.* 2008;49:480–508.
13. Tashiro M, Fujimoto T, Itoh M, et al. ^{18}F-FDG PET imaging of muscle activity in runners. *J Nucl Med.* 1999;40:70–76.
14. Aoki J, Endo K, Watanabe H, et al. FDG-PET for evaluating musculoskeletal tumors: a review. *J Orthop Sci.* 2003;8:435–441.
15. Yeung HWD, Grewal RK, Gonen M, Schoder H, Larson SM. Patterns of ^{18}F-FDG uptake in adipose tissue and muscle: a potential source of false-positives for PET. *J Nucl Med.* 2003;44:1789–1796.